Article

Geological Controls on Mineralogy and Geochemistry of an Early Permian Coal from the Songshao Mine, Yunnan Province, Southwestern China

Ruixue Wang [1,2]

[1] College of Geoscience and Surveying Engineering, China University of Mining and Technology (Beijing), Beijing 100083, China; wangruixue504@gmail.com; Tel.: +86-10-8232-0638

[2] State Key Laboratory of Coal Resources and Safe Mining, China University of Mining and Technology (Beijing), Beijing 100083, China

Abstract: This paper discusses the content, distribution, modes of occurrence, and enrichment mechanism of mineral matter and trace elements of an Early Permian coal from Songshao (Yunnan Province, China) by means of coal-petrological, mineralogical, and geochemical techniques. The results show that the Songshao coal is characterized by high total and organic sulfur contents (3.61% and 3.87%, respectively). Lithium (170.39 µg/g) and Zr (184.55 µg/g) are significantly enriched in the Songshao coal, and, to a lesser extent, elements such as Hg, La, Ce, Nd, Th, Sr, Nb, Sn, Hf, V, and Cr are also enriched. In addition to Hg and Se that are enriched in the roof and floor strata of the coal seam, Li, La, Ce, Pr, Nd, Sm, Gd, Y, Cd, and Sb are slightly enriched in these host rocks. Compared to the upper continental crust, rare earth elements and yttrium in the host rocks and coal samples are characterized by a light-REE enrichment type and have negative Eu, positive Ce and Gd anomalies. Major minerals in the samples of coal, roof, and floor are boehmite, clay minerals (kaolinite, illite, and mixed layer illite-smectite), pyrite, and anatase. Geochemical and mineralogical anomalies of the Songshao coal are attributed to hydrothermal fluids, seawater, and sediment-source rocks.

Keywords: coal; mineral; elements; Early Permian; genetic types

1. Introduction

Yunnan is one of the most coal-rich provinces in Southern China. Coal resources are mainly concentrated in the east and south of Yunnan. The Songshao Mine is located in the eastern part of Yunnan Province (Figure 1). Previous studies have focused on geologic structure, coal-bearing sequences, and coal quality of the Songshao Mine [1]. This paper aims to discuss geological controls on mineralogy and geochemistry of Early Permian coal from the Songshao Mine. Studies on mineral matter in coal are important because the process of coal formation, including peat accumulation, the interaction of the organic matter with basinal fluids, sediment diagenesis, and sometimes synsedimentary volcanic inputs, may result in enrichment of mineral matter in coal. Therefore, investigations on the mineral matter in coal could help to better understand the process of coal formation [2–4]. From an economic perspective, mineral matter in coal can serve as carriers for some valuable elements (e.g., Ga, Al, rare earth elements and yttrium) that have been recovered, or have such potential, from coal combustion wastes [5–8]. Geochemical anomalies in coals from Eastern Yunnan have previously been reported; for instance, Zhou et al. [9] reported trace-element geochemistry of altered volcanic ash layers (tonsteins) in Late Permian coal-bearing sequences in Eastern Yunnan and Western Guizhou Provinces; Dai et al. [10] described modes of occurrence and origin of quartz and chamosite in Xuanwei coals. Dai et al. [11] found a new type of Nb(Ta)–Zr(Hf)–REE–Ga polymetallic

deposit of volcanic origin in the Late Permian coal-bearing strata of Eastern Yunnan; Dai et al. [12] reported on the mineralogical and geochemical compositions of Late Permian C2 and C3 coals (both medium-volatile bituminous) from the Xinde Mine in Xuanwei, Eastern Yunnan. Geological factors controlling these geochemical and mineralogical anomalies have previously been analyzed [3,13–16]. For example, Dai et al. [13] documented mineralogical and geochemical anomalies of Late Permian coals from the Fusui coalfield, which were caused by influences from terrigenous materials and hydrothermal fluids.
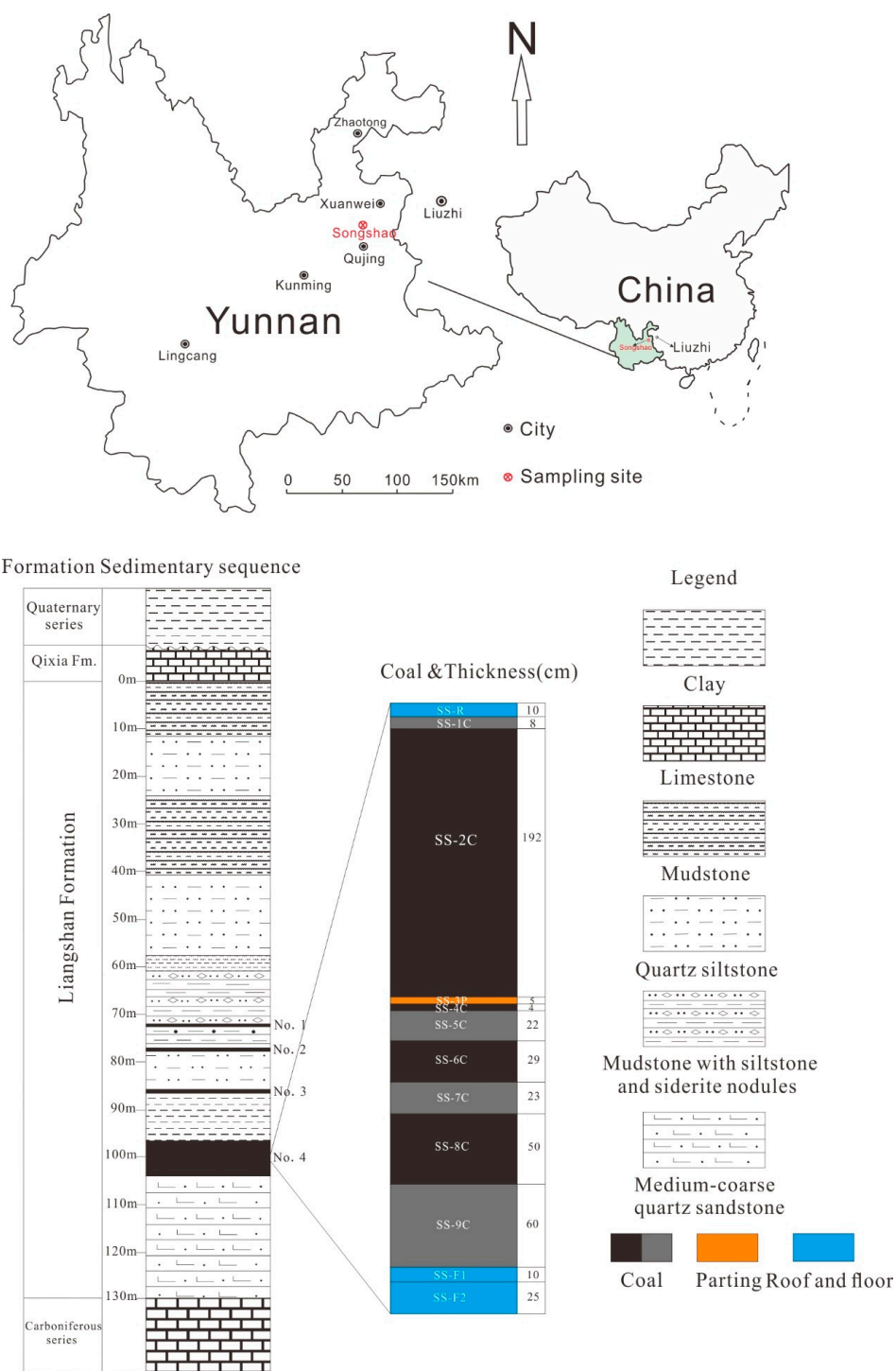

Figure 1. Location and sedimentary sequence of the Songshao Mine, Eastern Yunnan Province, China.

In the present study, new data on the Early Permian Coal from Songshao are reported with the aim to: (1) investigate geochemical and mineralogical compositions and modes of occurrence of elements and minerals; and (2) discuss the geological factors influencing mineralogical and geochemical anomalies.

2. Geological Setting

The sedimentary sequences in the Songshao Mine include Upper Carboniferous strata, Lower Permian Liangshan Formation, Lower Permian Qixia Formation, and the Quaternary system (Figure 1).

The Liangshan Formation comprises the coal-bearing seam, which underlies limestone of the Qixia Formation, and conformably overlies Carboniferous limestone. The lower part of the Liangshan Formation consists of coarse quartzose sandstones; the middle part is mainly composed of mudstones, interlayered with coal seams; and the upper part of the formation consists mainly of mudstones interbedded with quartzose sandstones. The thickness of the Liangshan Formation is about 131 m, and the coal seams are numbered 1 to 4. Only the No. 4 coal seam is minable and contains several gritty mudstone partings. The thickness of the No. 4 coal varies from 2 to 6 m. Samples, taken from No. 4 coal bed were numbered as SS-R, SS-1C, SS-2C, SS-3P, SS-4C, SS-5C, SS-6C, SS-7C, SS-8C, SS-9C, SS-F1 and SS-F2 (SS-R is roof; SS-3P is parting, SS-F1 and SS-F2 are floors and others are coals).

The roof of No. 4 coal is made up of grey black carbonaceous mudstone, and the floor consists of quartzose sandstones. The Upper Carboniferous Formation is made up of dolomite limestone. The Qixia Formation consists of medium-thick and thick limestone. The Quaternary system is composed of colluvial deposits.

3. Samples and Analytical Procedures

The samples selected for this study were collected from the faces of the mined coal seams in the Songshao Mine (No. 4 coal; Figure 1). All collected samples were immediately stored in plastic bags to minimize contamination and oxidation.

All the analyses were conducted at the State Key Laboratory of Coal Resources and Safe Mining (China University of Mining and Technology, Beijing, China). Proximate analysis was performed according to Chinese Standard GB/T 212-2008 [17]. The total sulfur and forms of sulfur were conducted following Chinese Standard GB/T 214-2007 [18] and GB/T 215-2003 [19], respectively. Mean random vitrinite reflectance (R_r) and maceral composition followed ISO 7404-5: 2009 [20]. Percentages of major-element oxides were determined by X-ray fluorescence (XRF) spectrometry (Thermofisher ARL Advant'XP+, ThermoFisher Scientific, Waltham, MA, USA). Trace-element concentrations were determined by inductively coupled plasma mass spectrometry (ICP-MS, Thermofisher X series II, Thermo Fisher Scientific), with exception of Hg and F. Mercury was determined using a Milestone DMA-80 Hg analyzer (Milestone, Sorisole, Italy), with a detection limit of 0.005-ng Hg, 1.5% relative standard deviation (RSD), and 0–1000 ng linearity for the calibration [21]. Fluorine was determined by pyrohydrolysis in conjunction with an ion-selective electrode, following the method described in Chinese National Standard GB/T 4633-1997 (1997) [22]. The mineralogy was determined by X-ray powder diffraction (XRD, Rigaku, Tokyo, Japan) plus Siroquant™ (Sietronics Pty Ltd, Canberra, Australia), optical microscopic observation, and a Field Emission-Scanning Electron Microscope (FE-SEM, FEI Quanta™ 650 FEG, Hillsboro, OR, USA), in conjunction with an energy-dispersive X-Ray spectrometer(EDS, Genesis Apex 4, EDAX Inc., Mahwah, NJ, USA), and these analytical procedures were described by Dai et al. [13].

4. Results

4.1. Ultimate and Proximate Analyses and Coal Rank

The vitrinite reflectance (1.24%) and volatile matter (30.91 wt %, daf) of the coal bench samples (Table 1) indicate a middle- to high-volatile bituminous rank, according to the ASTM classification

(ASTM D388-12, 2012) [23]. The coal is a medium-ash and high-sulfur coal according to Chinese Standards GB/T 15224.1-2004 [24] (coals with ash yield 20.01%–30.00% are high-ash coal) and GB/T 15224.2-2004 [25] (coals with total sulfur content >3% are high-sulfur coal). Organic sulfur accounts for most of the otal sulfur (Table 1). However, sample SS-1C has a higher content of pyrite sulfur than other coal benches.

Table 1. Proximate and ultimate analyses (wt %), and forms of sulfur (wt %) in Songshao coal.

Sample	R_r	M_{ad}	A_d	VM_{daf}	$S_{t,d}$	$S_{s,d}$	$S_{p,d}$	$S_{o,daf}$	N_{daf}	C_{daf}	H_{daf}
SS-R	nd	nd	79.88	nd	5.35	nd	nd	nd	nd	nd	nd
SS-1C	1.35	1.40	33.35	29.84	13.03	0.31	8.06	6.99	0.70	75.50	4.04
SS-2C	1.21	0.64	19.22	30.68	3.85	0.05	0.71	3.83	1.10	85.25	4.84
SS-3P	1.17	0.47	47.19	77.10	1.68	0.20	0.04	2.72	0.62	64.71	3.16
SS-4C	1.26	0.63	9.67	27.66	3.78	bdl	0.11	4.09	1.16	87.57	4.73
SS-5C	1.29	0.59	26.35	28.84	2.86	bdl	0.05	3.84	1.21	84.75	4.98
SS-6C	1.23	0.52	24.20	29.81	2.83	bdl	0.07	3.68	1.11	84.97	4.93
SS-7C	1.41	0.44	17.84	28.31	3.26	0.01	0.10	3.83	0.98	86.05	4.82
SS-8C	1.22	0.58	32.77	31.62	2.81	bdl	0.47	3.55	1.11	83.36	5.18
SS-9C	1.24	0.52	29.85	29.87	3.16	0.07	0.25	4.04	1.01	83.63	4.97
SS-F1	nd	nd	50.33	nd	1.53	nd	nd	nd	nd	nd	nd
SS-F2	nd	nd	80.78	nd	0.45	nd	nd	nd	nd	nd	nd
WA	1.24	0.60	23.80	30.91	3.61	0.04	0.62	3.87	1.07	84.32	4.88

M, moisture; A, ash yield; VM, volatile matter; C, carbon; H, hydrogen; N, nitrogen; S_t, total sulfur; S_s, sulfate sulfur; S_p, pyrite sulfur; S_o, organic sulfur; ad, air-dry basis; d, dry basis; daf, dry and ash-free basis; WA, weighted average for coals (weighted by thickness of sample interval); bdl, below detection limit; nd, not detected.

4.2. Geochemical Composition

4.2.1. Major Element Oxides

The major-element oxides are mainly represented by SiO_2 and Al_2O_3 (Table 2). When considered on a whole-coal basis, Songshao coal contains higher proportions of Al_2O_3, SiO_2, and, to a lesser extent, MgO, TiO_2, and K_2O, than the average values for Chinese coals reported by Dai et al. [26]; other major element oxides, however, are either lower than, or close to, corresponding average values for Chinese coals. The SiO_2/Al_2O_3 ratios for the coals are much lower than those of common Chinese coals (1.42) [26] and the theoretical SiO_2/Al_2O_3 ratio of kaolinite (1.18).

Table 2. Percentages of major-element oxides in the Songshao coal, parting, roof and floor rocks.

Sample	Th (cm)	LOI	SiO_2	TiO_2	Al_2O_3	Fe_2O_3	MnO	MgO	CaO	Na_2O	K_2O	P_2O_5	SiO_2/Al_2O_3
SS-R	10	20.12	40.27	0.86	28.27	6.41	0.01	1.03	0.35	0.05	2.15	0.06	1.42
SS-1C	8	66.65	9.08	0.2	8.73	13.83	0.01	0.13	0.14	0.04	0.11	0.2	1.04
SS-2C	192	80.78	8.35	0.46	8.07	0.9	0	0.14	0.37	0.03	0.1	0.12	1.03
SS-3P	5	52.81	0.76	0.02	1.6	0.59	0.08	0.26	36.97	0.02	0	0.01	0.48
SS-4C	4	90.33	3.07	0.13	4.8	0.2	0	0.18	0.41	0.19	0.03	0.03	0.64
SS-5C	22	73.65	11.55	0.44	13.08	0.19	0	0.36	0.1	0.04	0.19	0.03	0.88
SS-6C	29	75.8	10.36	0.42	12.28	0.22	0	0.3	0.07	0.02	0.19	0.02	0.84
SS-7C	23	82.16	7.72	0.29	8.86	0.13	0	0.27	0.1	0.02	0.13	0.03	0.87
SS-8C	50	67.23	14.57	0.57	15.75	0.61	0	0.4	0.11	0.03	0.33	0.06	0.93
SS-9C	60	70.15	13.72	0.54	13.74	0.66	0	0.31	0.08	0.02	0.42	0.03	1
SS-F1	10	49.67	25.24	1.12	22.83	0.19	0	0.21	0.07	0.01	0.39	0.03	1.11
SS-F2	25	19.22	39.79	1.65	37.45	0.46	0	0.31	0.05	0.01	0.64	0.06	1.06
SS Coal	-		76.5	10.24	0.46	10.56	0.95	0	0.23	0.23	0.03	0.19	0.08	0.97
Chinese Coal [a]	n.d.	n.d.	8.47	0.33	5.98	4.85	0.02	0.22	1.23	0.16	0.19	0.09	1.42
CC	n.d.	n.d.	1.21	1.4	1.77	0.2	0.15	1.06	0.19	0.18	1.01	0.88	0.68

Th, thickness; LOI, loss on ignition; CC, weighted average for coal samples; [a] From Reference [26]; n.d., no data.

The content of Fe_2O_3 is significantly higher in the roof and sample SS-1C than in other samples. The content of CaO in the parting SS-3P is particularly high. Based on the variation in concentrations through the seam section, two groups of major element oxides can be classified:

Group 1 includes SiO_2, TiO_2, Al_2O_3, and K_2O, all of which show a saw-like distribution, similar to the ash yield variation through the seam section. These oxides are enriched in the host rocks (roof and floor), but are at a low level in the coal benches and parting (Figure 2).

Group 2 consists of Na_2O, MgO, P_2O_5, MnO, and Fe_2O_3. The concentrations of these oxides do not show distinct variation through the seam section.
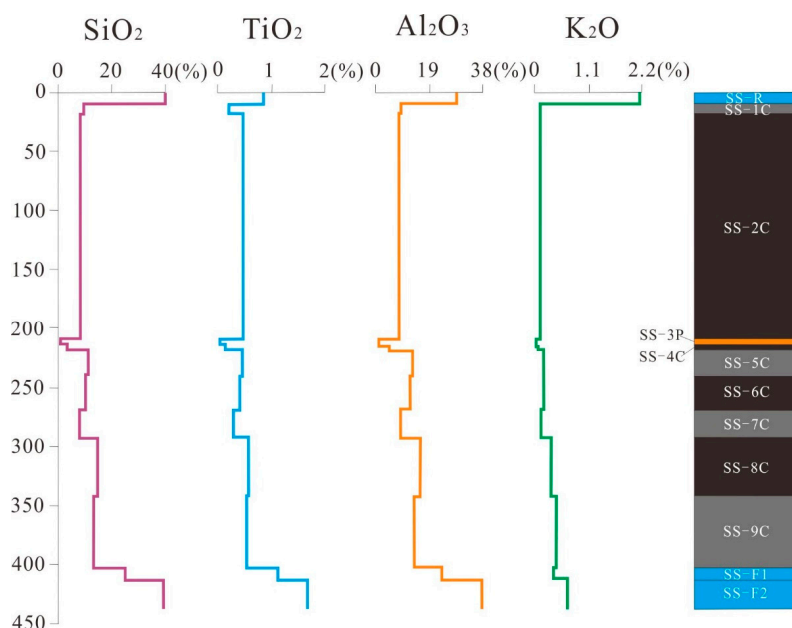

Figure 2. Variations of SiO_2, TiO_2, Al_2O_3 and K_2O through the seam section.

4.2.2. Trace Elements

The trace-element contents of Songshao coal are listed in Table 3. Compared to the averages for world hard coals [27], and based on the enrichment classification of trace elements in coal by Dai et al. [28], a number of trace elements are enriched in Songshao coal. Lithium has a concentration coefficient (CC: ratio of element concentration in Songshao coals vs. world hard coals) >10. Zirconium displays CC values between 5 and 10. Elements, including Hg, Sr, Nb, Sn, Hf, V, Cr, Se, Th, and some light rare earth elements (La, Ce, and Nd), are slightly enriched in the coal (CC = 2–5). However, Rb, Ba, Bi, Mo, and Sb, are depleted in the coal (CC < 0.5). The concentrations of the remaining elements (0.5 < CC < 2) are close to the corresponding averages for world hard coals [27].

Particularly, a number of trace elements are enriched in sample SS-1C. Trace elements with a concentration coefficient >10 include Hg (CC = 19.73) and V (CC = 13.69); trace elements with a CC of 5–10 include Sc, La, Ce, Pr, Sm, Eu, Th, Li, Sr, Se, Zr, Cr, and Tl.

Trace elements in the roof and floor rocks with a concentration coefficient (CC = ratio of element concentration in Songshao coal vs. UCC) higher than 10 include Hg and Se. Lithium shows a CC of 5–10. Lanthanum, Ce, Pr, Nd, Sm, Gd, Y, Cd, and Sb are slightly enriched in the roof and floor samples (CC = 2–5).

The anomalous geochemical composition of Songshao coal is represented by ratios of some trace elements. On average, Songshao coal has higher Nb/Ta, Zr/Hf, and especially Li/Rb values, as well as lower values of Ba/Sr and Rb/Cs than the averages for the world hard coals. From top (roof) to bottom (floor), the ratios of Ba/Sr and Nb/Ta show similar distribution patterns, which gradually increase; the ratio of Rb/Cs, however, shows an adverse trend.

Table 3. Trace-element concentrations (μg/g) in the Songshao coal, parting, and roof and floor rocks.

Sample	SS-R	SS-1C	SS-2C	SS-3P	SS-4C	SS-5C	SS-6C	SS-7C	SS-8C	SS-9C	SS-F1	SS-F2	World	SC	C1	UCC	PC	C2
Li	160.70	84.29	140.24	17.10	72.32	170.02	184.16	124.26	231.48	257.89	844.97	944.01	14.00	170.39	12.17	20.00	116.01	5.80
Be	3.45	3.29	0.98	0.37	0.78	1.88	1.87	1.30	1.89	1.92	3.24	3.19	2.00	1.41	0.71	3.00	1.62	0.54
F	670.30	138.20	131.09	49.00	154.90	176.81	175.67	158.68	204.91	174.03	165.51	293.06	82.00	153.84	1.88	-	348.55	-
Sc	25.53	25.02	3.81	1.61	7.10	5.07	6.41	4.13	4.06	6.87	10.47	30.63	3.70	5.03	1.36	11.00	4.57	0.42
V	231.22	383.34	57.25	9.74	34.93	76.15	72.88	55.08	88.81	99.12	231.22	120.60	28.00	75.55	2.70	60.00	59.02	0.98
Cr	149.02	87.56	35.44	6.44	19.58	41.68	36.16	34.45	43.83	54.30	149.02	111.25	17.00	40.26	2.37	35.00	32.18	0.92
Co	20.24	19.44	5.76	6.38	3.70	3.28	2.23	4.35	2.78	2.92	20.24	2.46	6.00	4.73	0.79	10.00	5.17	0.52
Ni	55.07	34.39	14.59	11.27	6.26	20.50	14.34	15.10	23.40	27.39	55.07	38.61	17.00	18.28	1.08	20.00	17.84	0.89
Cu	60.63	20.57	23.98	3.82	23.53	34.69	32.71	34.61	47.51	32.42	60.63	17.88	16.00	29.80	1.86	25.00	25.00	1.00
Zn	150.53	9.04	2.42	11.40	0.60	2.88	2.93	3.77	9.96	7.09	150.53	8.69	28.00	4.46	0.16	71.00	12.65	0.18
Ga	50.30	15.91	7.43	1.10	3.98	10.80	9.00	10.02	11.37	14.08	36.39	24.71	6.00	9.46	1.58	17.00	8.26	0.49
Ge	1.46	0.84	1.64	0.15	0.24	0.65	0.88	1.32	1.11	0.98	0.86	1.28	2.40	1.29	0.54	1.60	1.68	1.05
As	9.34	12.31	2.87	1.06	2.11	1.53	1.40	1.51	2.79	4.02	2.18	2.25	9.00	2.96	0.33	2.00	3.81	1.91
Se	7.22	9.17	4.16	0.94	4.60	5.53	6.18	4.08	7.01	6.22	3.90	2.61	1.60	5.18	3.24	0.08	3.92	47.23
Rb	96.10	3.71	1.97	0.09	0.55	2.77	2.71	1.97	4.43	4.02	2.94	4.34	18.00	2.69	0.15	112.00	8.02	0.07
Sr	104.84	588.93	493.21	180.81	139.62	22.06	22.96	16.11	31.17	17.25	19.01	10.42	100.00	267.14	2.67	350.00	209.03	0.60
Zr	209.44	227.44	219.24	7.06	40.47	151.48	136.14	93.08	178.18	168.14	422.17	589.72	36.00	184.55	5.13	190.00	132.90	0.70
Nb	18.43	4.15	8.89	0.94	2.56	8.21	8.15	5.82	8.51	7.56	21.85	32.61	4.00	8.10	2.03	25.00	6.68	0.27
Mo	0.69	2.08	0.39	0.14	0.22	1.77	0.50	0.57	0.80	0.73	0.88	1.23	2.10	0.62	0.29	1.50	1.13	0.76
Ag	0.97	1.29	1.18	bdl	0.17	0.83	0.76	0.44	0.96	0.97	0.97	2.54	bdl	1.00	bdl	0.05	0.65	13.07
Cd	0.53	0.56	0.29	0.05	0.19	0.30	0.28	0.23	0.63	0.50	0.53	0.67	0.20	0.36	1.81	0.10	0.31	3.05
In	0.19	0.10	0.04	0.13	0.02	0.05	0.04	0.05	0.06	0.09	0.25	0.13	0.04	0.05	1.30	-	0.05	-
Sn	4.97	5.12	2.54	38.34	0.68	2.02	1.51	2.50	2.16	6.26	8.68	5.73	1.40	3.45	2.46	5.50	2.73	0.50
Sb	0.97	0.62	0.26	0.12	0.23	0.37	0.30	0.18	0.46	0.51	0.47	0.66	1.00	0.33	0.33	0.20	0.57	2.83
Cs	15.02	0.69	0.36	0.14	0.12	1.51	1.14	0.77	2.08	2.72	3.13	3.44	1.10	1.09	0.99	3.70	1.09	0.29
Ba	131.56	77.11	24.02	6.63	5.59	10.54	7.81	6.70	15.72	16.17	10.38	5.04	150.00	19.47	0.13	550.00	64.86	0.12
La	100.65	29.82	5.99	25.27	34.61	36.14	23.61	45.01	36.70	60.67	102.44	57.28	11.00	34.27	3.12	30.00	83.12	2.77
Ce	185.72	58.81	12.06	41.35	77.86	80.91	54.56	95.52	88.70	120.63	240.78	110.15	23.00	72.30	3.14	64.00	185.05	2.89
Pr	18.18	5.23	1.41	4.04	6.98	7.77	5.11	8.88	8.64	14.30	17.93	12.74	3.40	6.70	1.97	7.10	15.97	2.25
Nd	68.89	18.92	5.82	14.89	25.38	29.32	19.84	32.67	33.62	54.74	68.81	47.63	12.00	24.91	2.08	26.00	60.98	2.35
Sm	11.82	3.02	1.10	2.61	3.95	4.93	3.44	5.13	5.92	9.47	11.40	7.43	2.20	4.10	1.86	4.50	10.09	2.24
Eu	2.44	0.53	0.21	0.46	0.71	0.88	0.59	0.87	1.07	1.59	1.73	1.25	0.43	0.73	1.70	0.90	1.59	1.77
Gd	11.63	3.42	1.30	2.90	4.55	5.37	3.51	5.37	6.23	9.76	10.35	7.14	2.70	4.44	1.65	3.80	9.50	2.50
Tb	1.10	0.38	0.16	0.36	0.48	0.59	0.38	0.55	0.72	1.20	1.26	0.80	0.31	0.49	1.57	0.60	1.14	1.90
Dy	5.30	2.14	0.87	1.97	2.61	3.10	1.98	2.68	3.91	6.74	6.77	4.69	2.10	2.61	1.24	3.50	6.30	1.80
Y	25.96	10.69	5.05	10.31	13.23	15.34	9.04	12.34	18.96	37.75	56.89	25.90	8.40	12.79	1.52	22.00	45.75	2.08

Table 3. *Cont.*

Sample	SS-R	SS-1C	SS-2C	SS-3P	SS-4C	SS-5C	SS-6C	SS-7C	SS-8C	SS-9C	SS-F1	SS-F2	World	SC	C1	UCC	PC	C2
Ho	1.02	0.41	0.16	0.37	0.47	0.56	0.35	0.47	0.71	1.23	1.19	0.91	0.57	0.48	0.85	0.80	1.14	1.42
Er	3.20	1.26	0.48	1.12	1.40	1.67	1.00	1.34	2.08	3.62	3.49	3.02	1.00	1.45	1.45	2.30	3.42	1.49
Tm	0.44	0.18	0.06	0.15	0.18	0.22	0.13	0.17	0.27	0.45	0.44	0.43	0.30	0.20	0.65	0.30	0.44	1.46
Yb	3.26	1.28	0.40	1.08	1.27	1.56	0.88	1.16	1.88	3.06	2.96	3.19	1.00	1.38	1.38	2.20	3.03	1.38
Lu	0.46	0.17	0.05	0.15	0.16	0.20	0.12	0.15	0.25	0.40	0.39	0.45	0.20	0.18	0.91	0.30	0.40	1.34
Hf	5.34	3.83	5.56	0.21	1.12	4.25	3.83	2.48	4.76	4.75	10.00	13.78	1.20	4.81	4.01	5.80	3.55	0.61
Ta	1.28	0.36	0.70	0.29	0.17	0.59	0.59	0.38	0.42	0.27	1.41	2.15	0.30	0.55	1.83	2.20	0.46	0.21
W	5.17	0.24	1.20	0.14	0.16	0.56	0.50	0.62	0.58	0.66	2.65	11.90	0.99	0.87	0.88	2.00	0.91	0.46
Hg	0.26	1.97	0.17	0.02	0.12	0.14	0.13	0.10	0.21	0.24	0.17	0.24	0.10	0.21	2.11	0.02	0.17	8.63
Tl	0.79	3.45	bdl	bdl	bdl	bdl	bdl	bdl	0.02	0.03	0.79	0.02	0.58	0.07	0.12	0.80	0.25	0.31
Pb	34.89	11.87	10.11	0.97	6.79	15.73	17.38	9.81	18.75	21.37	34.89	7.12	9.00	13.65	1.52	20.00	12.03	0.60
Bi	1.80	0.04	0.21	0.60	bdl	0.23	0.19	bdl	0.13	1.06	1.03	1.84	1.10	0.32	0.29	-	0.59	-
Th	25.72	16.97	10.34	0.99	5.22	7.90	9.60	7.37	10.36	11.75	20.28	38.40	3.20	10.16	3.17	10.70	7.74	0.72
U	5.62	3.91	2.25	0.48	1.18	3.70	3.24	2.92	3.96	4.09	8.27	8.69	1.90	2.94	1.55	2.00	2.58	1.29

World, world hard coals, from Ketris and Yudovich [27]; SC, weighted average for coal samples; C1, concentration coefficient of coal samples; UCC, upper continental crust; PC, weighted average for host rock; C2, concentration coefficient of host rock; -, without the data item.

4.2.3. Rare Earth Elements

Rare earth elements (REE) in coal are generally associated with minerals, especially clay minerals and phosphate, which are generally associated with ash yield [29]; in some cases, heavy rare earth elements are associated with the organic matter in coal [30]. A threefold classification of REE was used for this study: Light (LREE: La, Ce, Pr, Nd, and Sm), medium (MREE: Eu, Gd, Tb, Dy, and Y), and heavy (HREE: Ho, Er, Tm, Yb, and Lu) REE [31]. Accordingly, in comparison with the upper continental crust [32], three enrichment types are identified [31]: L-type (light-REE; $La_N/Lu_N > 1$), M-type (medium-REE; $La_N/Sm_N < 1$ and $Gd_N/Lu_N > 1$), and H-type (heavy REE; $La_N/Lu_N < 1$).

With the exception of sample SS-9C, the REE patterns in the coal benches are characterized by L-REE enrichment, Eu negative anomalies, and Gd-maximum (Gd reaches to the peak of the patterns) (Figure 3). In particular, sample SS-1C has the highest REE concentration relative to other coal samples and does not show an Eu anomaly.
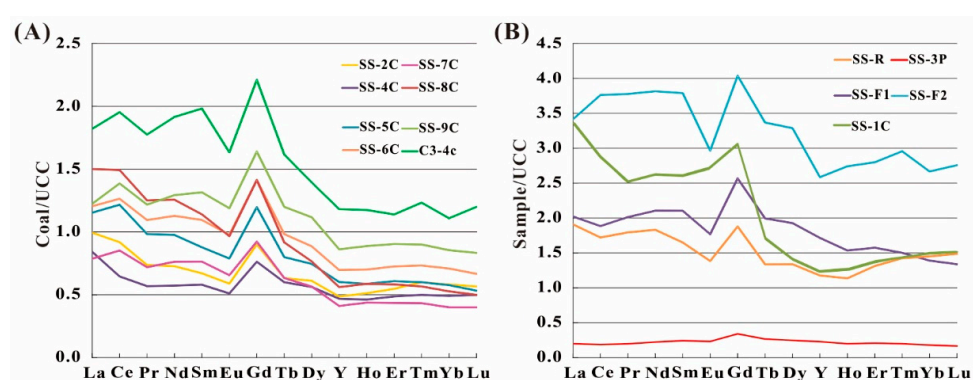
Figure 3. Distribution patterns of rare earth elements (REE) of samples in the Songshao coal mine. (**A**) Plots for the Songshao coal in comparison with C3-4c from the Xinde Mine. (**B**) Plots of SS-1C, roof and floor, and parting from the Songshao Coal Mine. REE are normalized by upper continental crust (Taylor and McLennan [32]).

The lower REE abundance of the parting is attributed to its lithological composition, which is represented by 97% calcite (Table 4). According to previous studies, the content of REE in limestone is lower in comparison with other lithology, such as clay and oil shale [33,34]. The REE distribution pattern for the parting is characterized by an M-REE enrichment type and almost no Eu anomalies.

Table 4. Low temperature ash (LTA) yields of coal samples and mineral compositions (%) of LTAs, parting, roof and floor determined by XRD and Siroquant. "-"means below the detection limit of Siroquant analysis.

Sample	LTA	Kaolinite	Illite	I/S	Marcasite	Pyrite	Calcite	Anatase	Boehmite	Diaspore	Brucite
SS-R	-	54.5	39.2	-	-	5.1	-	1.2	-	-	-
SS-1C	47.2	41.3	-	-	12.7	44.6	-	0.9	-	-	-
SS-2C	22.9	55.2	17.9	-	-	-	6.1	1.3	3.4	14.9	1.1
SS-3P	73.8	-	-	-	-	-	97.7	-	2.1	0.1	0
SS-4C	11.0	22.6	17.3	14.7	-	-	4.7	1.7	34.3	4.3	0.4
SS-5C	31.9	50.8	9.1	14.6	-	-	-	0.6	24.9	-	-
SS-6C	23.7	60.5	6.7	1.7	-	-	-	0.9	30.3	-	-
SS-7C	20.7	51.8	6.1	-	-	-	-	0.1	34.2	7.6	0.3
SS-8C	39.0	53.7	14.8	-	-	-	-	0.4	25.3	5.1	0.7
SS-9C	35.1	63.6	14.7	-	-	-	-	-	20.9	-	0.4
SS-F1	-	83.6	6.3	-	-	-	-	0.7	9.4	-	-
SS-F2	-	78.5	7.7	-	-	-	-	1.0	12.9	-	-

In addition, the floor and roof samples have similar REE distribution patterns, with weak negative Eu anomalies, and L- and M-REE enrichment types.

REE in all the samples are characterized by a Gd-maximum. The distribution patterns of REE in Songshao coal are similar to that in sample C3-4c from the Xinde Mine in Eastern Yunnan, China [12]. Sample C3-4c is characterized by M-type REE spectra with a Gd-maximum (Figure 3); such patterns in coal are typical of a great deal of acid water, including high pCO_2-waters in coal basins [35,36].

4.3. Mineralogical Composition

4.3.1. Mineral Phases

The proportions of each crystalline phase, identified from the X-ray diffractograms of the coal LTA (low temperature ash), parting, roof, and floor samples, are given in Table 4. The phases identified in the coal LTAs include kaolinite, illite, I/S (mixed layer of illite and smectite), marcasite, pyrite, calcite, anatase, boehmite, diaspore, and a trace amount of brucite. Additionally, stannite, fluorapatite, apatite, zircon, halotrichite, and some REE-bearing minerals, including xenotime, florencite, and silicorhabdophane, are also identified in sample SS-7C by SEM-EDS analysis.

Calcite is the dominant mineral in parting. Other minerals including boehmite and diaspore are also identified from parting LTA.

Minerals in the roof sample (SS-R) include kaolinite, illite, pyrite, and small proportions of anatase, quartz, and gypsum. The floors samples (SS-F1 and SS-F2) are composed of kaolinite, illite, anatase, and boehmite.

4.3.2. Comparison between Mineralogical and Chemical Compositions

The chemical composition of the (high-temperature) coal ash calculated from the XRD and Siroquant analyses of each LTA or roof and floor samples are listed in Table 4. The two data sets, derived respectively from the XRD and the XRF data, have been compared and are presented as *X*–*Y* plots (Figure 4), with a diagonal line on each plot indicating where the points would fall if the estimates from the two different techniques were equal. The points for SiO_2, and Al_2O_3 in Figure 4 plot close to the equality line, suggesting that the XRD results are generally compatible with the chemical analysis data.
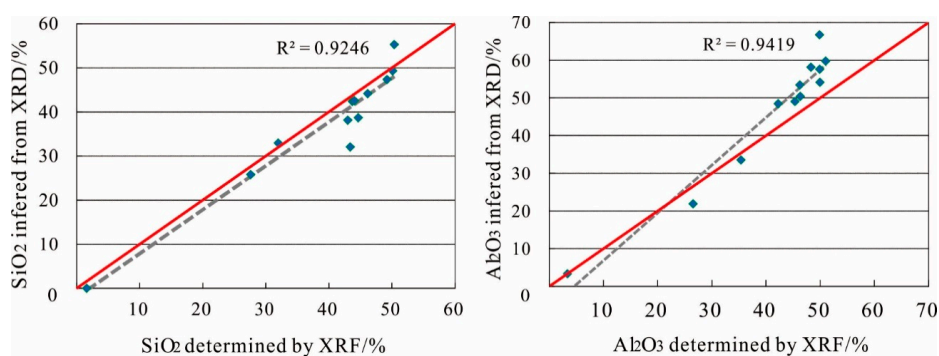
Figure 4. Comparison of observed normalized Si and Al oxide percentages from chemical analysis (*X*-axis) to oxide percentages for sample ash inferred from XRD analysis data (*Y*-axis). The diagonal line in each plot indicates equality.

4.3.3. Modes of Mineral Occurrence

Clay Minerals

Clay minerals, including kaolinite, I/S (mixed-layer illite-smectite), illite, and smectite, are identified using XRD and SEM-EDS. They normally occur in the matrix of organic matter of the coal (Figure 5A). Kaolinite is the dominant mineral both in the coals and the roof and floor strata. In some cases, kaolinite distributes along the bedding (Figure 5B), and sometimes it occurs in detrital forms.

Other modes of occurrence of kaolinite include fracture- and cell-fillings (Figure 5C) of authigenic origin [37]. I/S, illite, and smectite distribute along the bedding planes (Figure 5B); occur as cell-fillings (Figure 5D,E); or distribute around boehmite (Figure 5F).
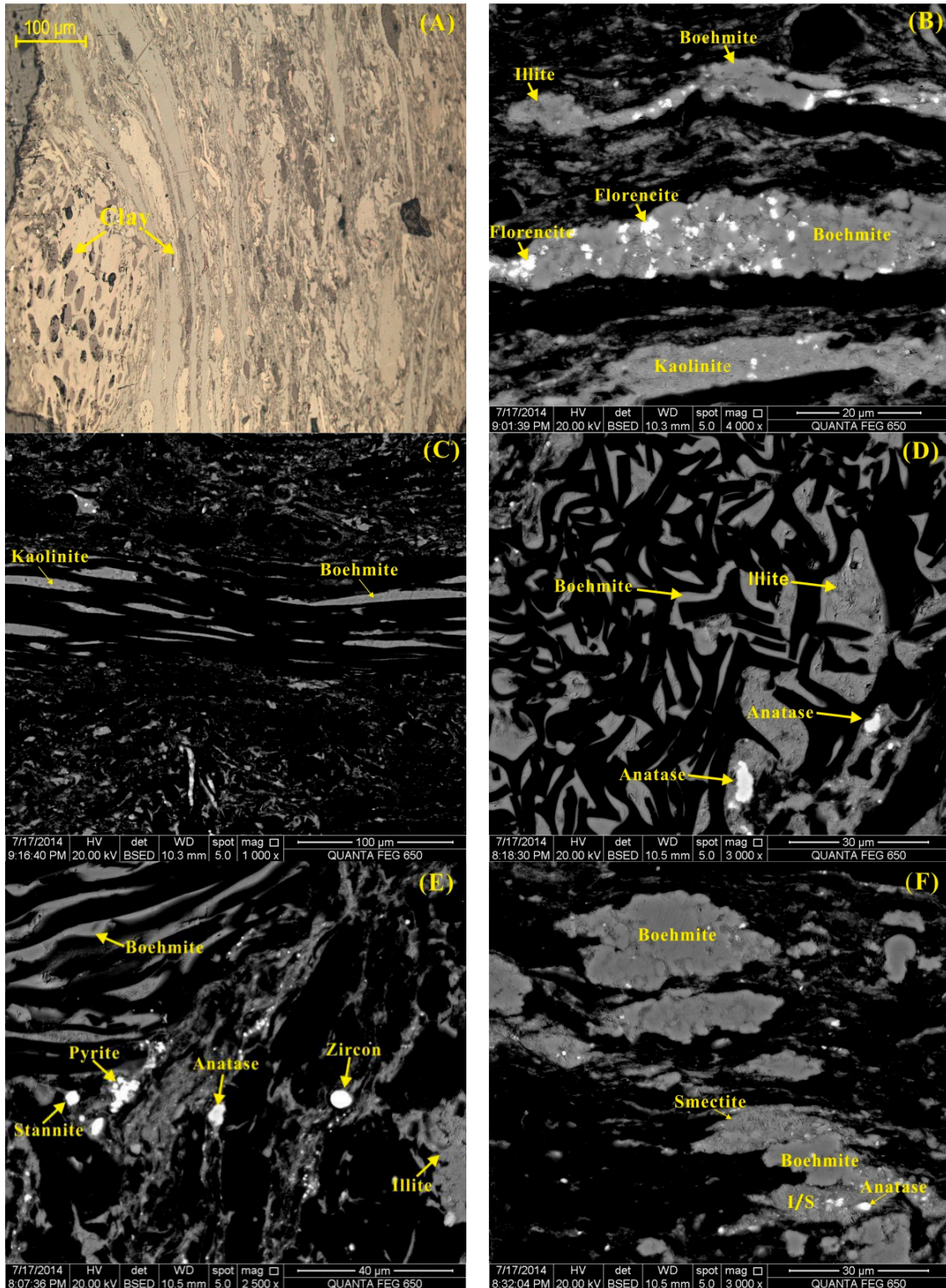

Figure 5. *Cont.*
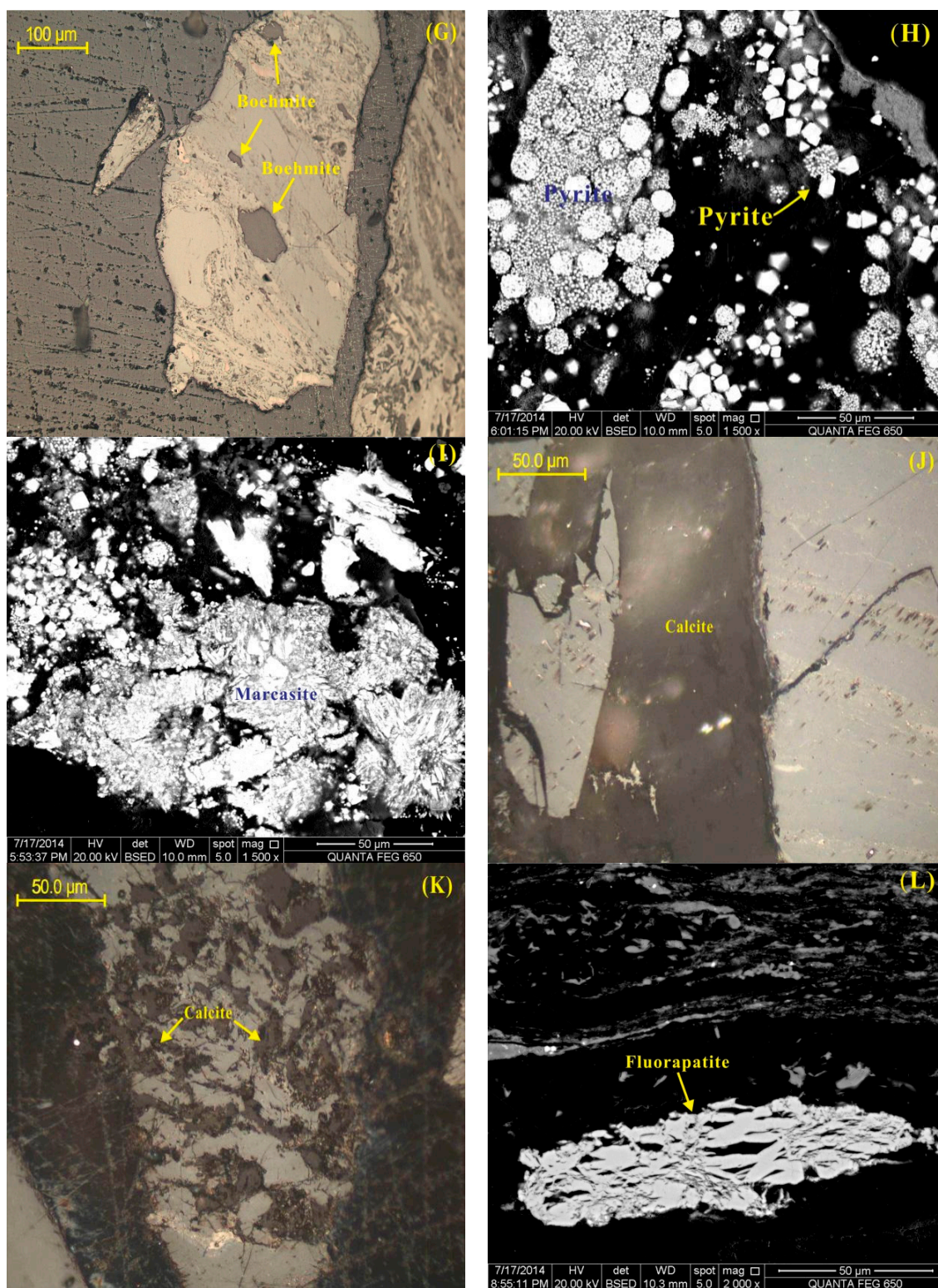
Figure 5. Minerals in the Songshao coal. (**A**) clay minerals in SS-9C; (**B**) kaolinite, illite, boehmite and florencite in SS-7C; (**C**) cell-filling kaolinite and boehmite in SS-7C; (**D**) cell-filling boehmite, illite, and anatase in SS-7C; (**E**) cell-filling boehmite, ditrital zircon, anatase, pyrite and stannite in SS-7C; (**F**) boehmite occurs small lumps and bead-like block embedded in the clay minerals and ditrital anatase in SS-7C; (**G**) boehmite in SS-9C; (**H**) framboidial pyrite in SS-1C; (**I**) plate, block and radial form marcasite in SS-1C; (**J**) vein-filling calcite in SS-3P; (**K**) cell-filling calcite in SS-3P; (**L**) fracture-filling florencite in SS-7C. B-F, H, I, L, SEM and back-scattered electron images; (**A**), (**G**), (**J**), (**K**), reflected light.

Boehmite, Disapore, Brucite

Oxyhydroxide minerals, such as boehmite, disapore, and brucite, were identified in Songshao coal. High boehmite content (mean 4.33%) was identified in Songshao coal, occurring as fracture-fillings (Figure 5B), small lumps (Figure 5F), cell-fillings (Figure 5D,E), and bead-like block embedded in the clay minerals (Figure 5F). The lumps show different shapes and variable sizes, from a few to one hundred micrometers. The surface of the boehmite in the coal is much smoother than that of the clay minerals (Figure 5F) and the relief of boehmite is higher under the polarizing microscope (Figure 5G). Minerals associated with the boehmite in the coal include goyazite, rutile, zircon, and Pb-bearing minerals (galena, clausthalite, and selenio-galena) [38]. Additionally, zircon is also identified in Songshao coal.

Pyrite and Marcasite

Pyrite is only detected in samples SS-R and SS-1C using the XRD technique. A trace amount of pyrite is also detected in sample SS-7C using SEM-EDS. Pyrite in sample SS-1C occurs as framboidal massive (Figure 5H) and euhedral crystal forms (Figure 5H), or distributes along the bedding (Figure 5E). Marcasite is only detected in sample SS-1C and coexists with pyrite, occurring as plate, block and radial forms (Figure 5I). This kind of marcasite may be of a syngenetic origin.

Calcite

Calcite is detected in samples SS-2C, SS-3P, and SS-4C using XRD and it accounts for 72.1% in the parting (SS-3P). Calcite occurs as vein- (Figure 5J), fracture- or cells-fillings (Figure 5K), indicating an epigenetic origin.

Antase and Zircon

Antase occurs as discrete particles in clay minerals (Figure 5E,F) or as cell-fillings (Figure 5D). Zircon occurs as detrital particles of terrigenous origin (Figure 5E).

The mode of occurrence of zircon indicates a detrital material of terrigenous origin. Zircon may be a pyroclastic mineral in some tonsteins [4,39] or it may occur as detrital material derived from the sediment source region.

Apatite, Halotrichite, and Stannite

Apatite in coal is classified as fluorapatite and zwiesellite. Fluorapatite is a common mineral in coal. It looks like bamboo leaves filling in the fracture (Figure 5L), indicating an epigenetic chemical deposition. A spot of halotrichite was also observed in sample SS-7C. The copiapite-group of minerals is one of the most common Fe-sulfates reported from many coals, such as coals from the Jaintia Hills coalfield in Meghalaya, India [40]. A trace of stannite was detected using SEM-EDS (Figure 5E).

REE-Bearing Minerals

REE-bearing minerals are at a low concentrations, below the detection limit of the XRD and Siroquant analysis, but were observed under SEM-EDS in sample SS-7C. These minerals are Xenotime, florencite, rhabdophane, and silicorhabdophane.

Phosphate minerals, such as apatite, monazite, and, in some cases, xenotime, zircon, and some clay minerals, are usually the carriers of thorium in coal [41]. In this study, thorium was not detected, but Dy was detected in xenotime.

Florencite occurs as fracture-fillings, coexisting with kaolinite (Figure 5B). However, the small size of these particles makes it difficult to obtain a representative EDS spectrum.

5. Factors Controlling Enrichment of Trace Elements and Minerals in Songshao Coal

It has been reported that seven factors control the enrichment of elements and minerals in Chinese coals: The sediment-source rocks, low-temperature hydrothermal fluids, marine environments,

volcanic ash, magmatic fluids, submarine exhalation, and groundwater [3]. The first three factors are likely to be responsible for the geochemical and mineralogical anomalies of Songshao coal.

5.1. Input from Sediment-Source Region

As described above, Songshao coal is enriched in Al, Si, Ti, Li, Zr, Hf, Th, Sr, and V. Aluminum and Si are largely contained in clay minerals. Two modes of kaolinite occurrence in Songshao coal were identified: Detrital kaolinite of terrigenous origin and cell-filling kaolinite of authigenic origin. Anatase, which occurs as discrete particles in the clay mineral matrix, is the host of Ti and was probably derived from sediment-source sources. Lithium generally occurs in minerals, or can be absorbed by bauxite minerals, which can then be named as a Li deposit [42] if Li is highly concentrated. Moreover, Li may occur in silicate minerals, because it tends to be absorbed by clay minerals, which are formed during a weathering process [43]. It was reported that the Langdaisa Li-bearing claystone of the Permian Liangshan Formation contains 0.12%–0.74% Li [44,45]. Langdaisa is located in the Liuzhi District of Guizhou and Liuzhi is situated to the northeast of the Songshao Mine, indicating the same sediment source for the Langdaisa Li-bearing claystone and Songshao coal. Thorium is not easily altered by the processes of weathering and transportation, and, thus, it can serve as an effective indicator for deducing the source region. Thorium is generally absorbed by clay and more likely occurs in bauxite [43]. In addition, thorium can occur in apatite, xenotime, or zircon in coal [41]. In this study, minerals including apatite, xenotime, and zircon have been identified in sample SS-7C by SEM-EDX; however, thorium was not found to occur in these minerals. The correlation coefficients of Zr-Th and Zr-Hf are 0.814 and 0.974, respectively (Figure 6). Zircon is the carrier of Zr and also contains Th and Hf. The mode of zircon occurrence indicates a detrital material of terrigenous origin. Elements Hf, Zr, and Li show a similar variation tendency through the seam section, suggesting a same source (Figure 6).
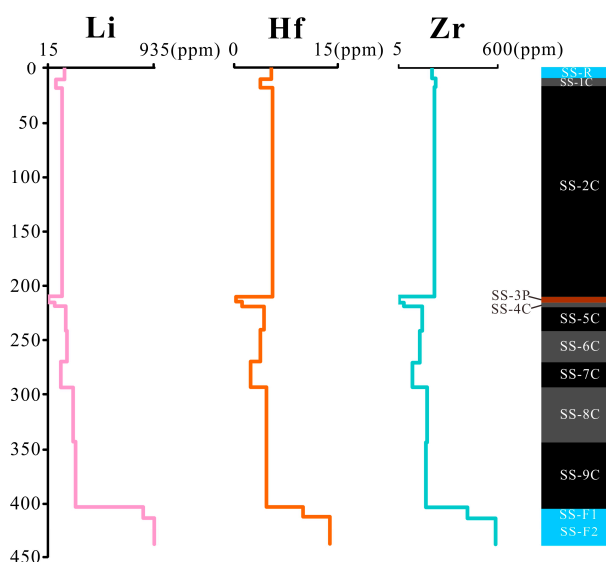

Figure 6. Variations of Li, Hf, and Zr through the seam section.

Seredin and Dai [31] suggested that the L-type distribution of REE in coal are attributed to terrigenous or tuffaceous origins during peat accumulation stage. In the first case, the REE may be transported as colloidal and ionic forms from uplift containing magmatic rocks enriched in light REE, such as granite and carbonatite [31]. The light REE enrichment type in Songshao coal indicates a terrigenous origin. A similar instance occurred in the No. 6 Coal seam in the Jungar deposit in Inner Mongolia, China [46]. REE are present in Songshao coal as REE-rich minerals, such as xenotime and florencite.

5.2. Hydrothermal Fluid Influences

Hydrothermal fluid is another critical factor responsible for the trace-element and mineral anomalies in the Songshao coal, parting, and roof and floor rocks. The hydrothermal fluid includes syngenetic hydrothermal solutions injected into the peat mire during peat accumulation. Mineralogical evidence of hydrothermal influence on Songshao coal includes:

(1) Pyrite and calcite occur as micro-veinlets (Figure 5H,J). Multi-generation pyrite occurs in sample SS-1C. Framboidal pyrite is of an early diagenetic origin [47]. It occurs as lenses and spheres and the aggregates are composed of microcrystalline paticles. The framboids are commonly coated by late-formed sulfides. Meanwhile, sample SS-1C is enriched in As, Se, and Hg. According to previous research [48–51], some trace elements, for instance, arsenic and mercury, are concentrated in the late stage of hydrothermal fluids. In some cases, arsenic was syngenetically derived from hydrothermal solutions [6]. Particularly, the enrichment of arsenic was associated with late-stage pyrite that coats early framboids and with microscale faulting. This phenomenon also occurred in the West Virginia coals from the Appalachian region, USA [52]. Therefore, hydrothermal fluid may be responsible for the enrichment of trace elements in sample SS-1C.

(2) Clay minerals, boehmite and calcite occur as cell-fillings (Figure 5B,C,K). Under favorable conditions, solutions that contained soluble Al and Si entered the coal basin, filled and then were deposited in the cells during peat accumulation.

(3) High boehmite content (mean 4.33%) in Songshao coal is not commonly observed; the content of boehmite in the coal present in this study is close to that (mean 6.1%) in the No. 6 Coal from the Jungar Coalfield [46] and from some mines of the Daqingshan Coalfield [53]. In addition, boehmite may be the result of low-temperature hydrothermal fluids, generally associated with zeolites [54]. However, zeolites have not been observed in the present study. The occurrence mode of boehmite in Songshao coal is similar to that in the No. 6 Coal in the Jungar Coalfield [46] and the Daqingshan Coalfield [53]. The boehmite in Jungar coals is the major carrier of Ga and Th, which are significantly enriched in the coal (44.8 µg/g Ga; 17.8 µg/g Th; on a whole coal basis). However, trace elements were not enriched with boehmite in Songshao coal. The difference in element abundance between boehmites in the coals from the different coalfields was probably due to different origins of boehmite. An explanation for high boehmite content is that in the humid–warm climatic conditions, rock in sediment source suffered from weathering and erosion, which can cause Al to be concentrated in weathering crust. Colloidal solution containing Al removed from the crust flowed into the peat mire, and boehmite was formed by compaction and dehydration of Al colloidal solution during peat accumulation and early diagenesis.

(4) The presence and mode of occurrence of xenotime, florencite, rhabdophane and silicorhabdophane in the coal present in this study indicate that these minerals were deposited from hydrothermal fluids at syngenetic or early diagenetic stages. Rhabdophane, florencite, and silicorhabdophane are the major carriers of light rare earth elements in the samples of the present study. These minerals in coal are generally derived from hydrothermal fluids, and they are also the major REE carriers in some other REE-rich coals as well [31,54–60].

(5) S positively correlates with Hg and Fe, with correlation coefficients $r_{S\text{-}Hg} = 0.85$ and $r_{S\text{-}Fe} = 0.88$ (Figure 7), respectively. Fluorine is slightly enriched in Songshao coal with CC = 1.88. Syngenetic hydrothermal solutions may be rich in Hg and F, and this could lead to enrichment of Hg in upper and lower portions of the coal seam and high F concentrations throughout the whole seam section. Hydrothermal fluids leading to enrichment of Hg and F has also been reported in some coals from other coalfields [61–64]. Fluorine-bearing fluorapatite was found to occur as fracture-fillings in sample SS-7C. Epigenetic hydrothermal fluids led to the enrichment of F, Fe, Se and S in the roof rock. Owing to the injection of epigenetic hydrothermal fluids into the coal seam, the concentrations of epithermal-associated elements (e.g., F, Se, S, and Hg) are highly elevated near the contact between the coal bench and roof strata.
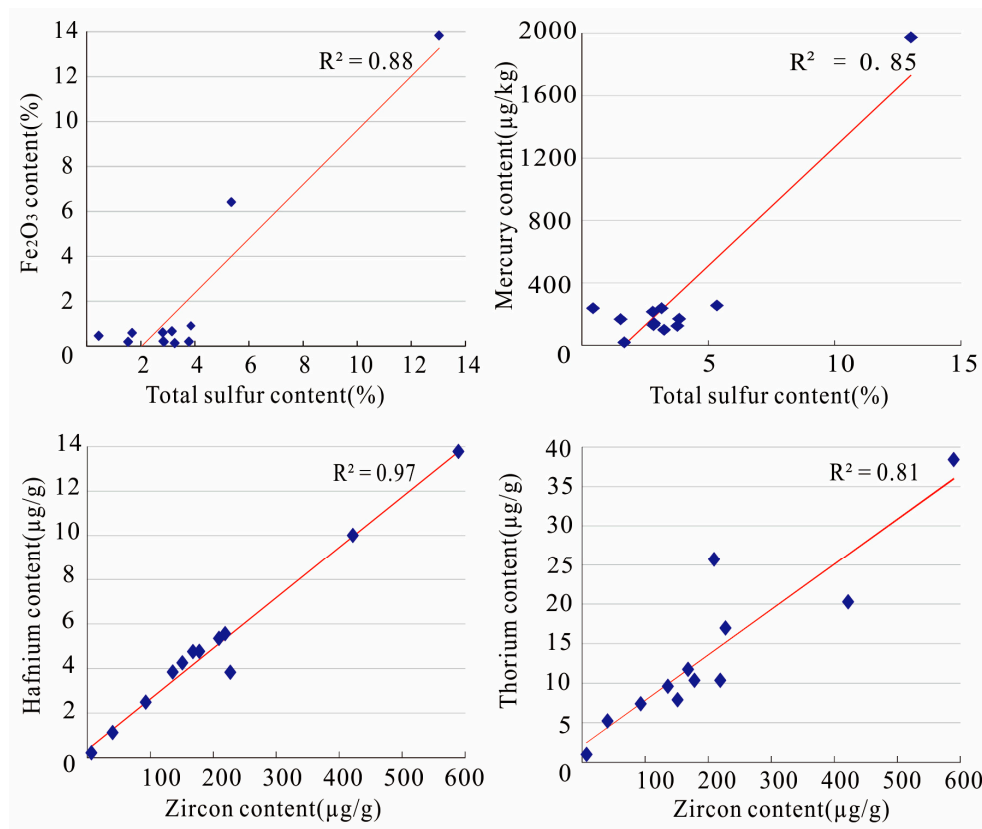
Figure 7. Correlation coefficients between two elements.

5.3. Marine Environments

Because Songshao is located in the area of arenaceous and argillaceous facies in litoral zone (Figure 8), the peat swamp of the coal had been subjected to a marine environment, as indicated by the following evidence:

(1) A number of researches showed that coals formed in marine-influenced environment are generally enriched in some elements, including S, B, V, Br, Rb, Sr, Mo, and U [65–69], because these elements are enriched in seawater in comparison with fresh water. Songshao coal, as described above, is enriched in V and Sr.

(2) Songshao coal is a high-sulfur coal with average total sulfur and organic sulfur contents 3.61% and 3.87%, respectively. Previous work showed that sulfate in seawater that flooded peat swamps is the major sources of sulfur for medium- and high-sulfur coals [70]. Some studies also indicated that submarine exhalation can also lead to sulfur enrichment in coal [71]. The elevated content of sulfur in Songshao coal is attributed to seawater that injected into the peat swamp during peat accumulation. Sulfates in the seawater were reduced by anaerobic sulfate-reducing bacteria. Various forms of sulfur, which decrease in interstitial water, react with iron ions and organic matters. Then, sulfur-bearing minerals (pyrite mostly) and organic sulfide formed [72].
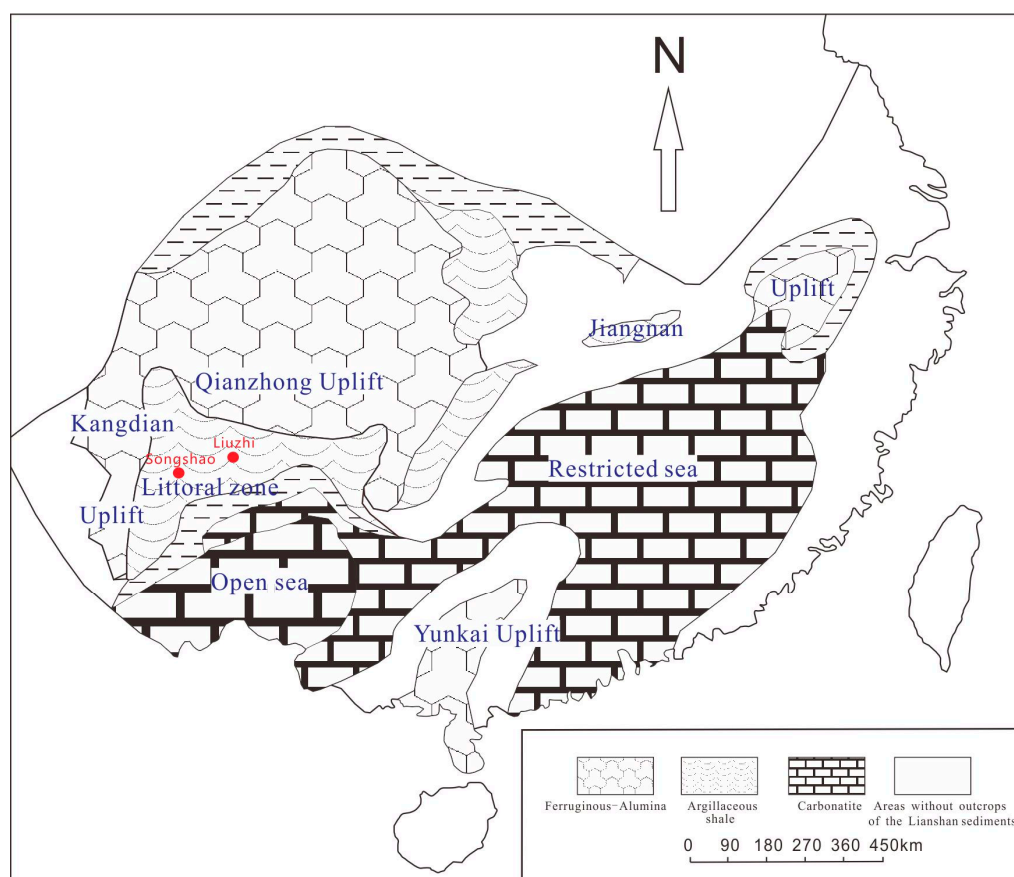
Figure 8. Sketch map of lithological facies and paleogeography in the study area during the Liangshan Stage. Modified from [73,74].

6. Conclusions

Songshao coal is medium- to high-volatile bituminous in rank, with high total and organic sulfur contents. Major-element oxides are mainly represented by SiO_2 and Al_2O_3. Trace elements, including Li, Zr, Hg, Sr, Nb, Sn, Hf, V, Cr, Se, Th, and some light REE, are enriched. The REE enrichment patterns in the coal seam are L-types (light REE enrich) and are characterized by negative Eu anomalies and a Gd-maximum. The mineral phases identified in the coal LTAs include kaolinite, illite, I/S (mixed layer illite-smectite), pyrite, calcite, anatase, boehmite, diaspore, and some REE-bearing minerals. Clay minerals occur in the matrix of organic matter. Boehmite in the coal occurs as fracture-fillings, small lumps, as cell-fillings, or as bead-like blocks embedded in the clay minerals. Pyrite occurs as framboidal forms; calcite occurs as fracture-fillings or cell-fillings. Other minerals occur as debris in the samples.

High total and organic sulfur contents and the enrichment Sr and V are attributed to a marine influence. Hydrothermal fluids are responsible for the high boehmite content (mean 4.33%) and its modes of occurrence; the presence and modes of REE-bearing minerals, pyrite and calcite; the enrichment of Hg and F in the coal, roof and floor strata rocks. Songshao coal and the roof and floor strata rocks are also enriched in SiO_2, Al_2O_3, Li, Zr, and light rare earth elements, which were derived from the sediment source.

Conflicts of Interest: The author declares no conflict of interest.

References

1. Yunnan Coal Geology Prospecting Team No. 143. *Report on Coal Geological Exploration of Songshao Mine*; Yunnan Coal Geology Prospecting Team No. 143: Qujing, China, 1996.

2. Dai, S.; Wang, X.; Zhou, Y.; Hower, J.C.; Li, D.; Chen, W.; Zhu, X.; Zou, J. Chemical and mineralogical compositions of silicic, mafic, and alkali tonsteins in the late Permian coals from the Songzao Coalfield, Chongqing, Southwest China. *Chem. Geol.* **2011**, *282*, 29–44. [CrossRef]

3. Ren, D.; Zhao, F.; Dai, S.; Zhang, J.; Luo, K. *Geochemistry of Trace Elements in Coal*; Science Press: Beijing, China, 2006; pp. 40–59. (In Chinese)

4. Ward, C.R. Analysis and significance of mineral matter in coal seams. *Int. J. Coal Geol.* **2002**, *50*, 135–168. [CrossRef]

5. Wang, X.; Dai, S.; Ren, D.; Yang, J. Mineralogy and geochemistry of Al-hydroxide/oxyhydroxide mineral-bearing coals of Late Paleozoic age from the Weibei coalfield, southeastern Ordos Basin, North China. *Appl. Geochem.* **2011**, *26*, 1086–1096. [CrossRef]

6. Dai, S.; Wang, X.; Seredin, V.V.; Hower, J.C.; Ward, C.R.; O'Keefe, J.M.K.; Huang, W.; Li, T.; Li, X.; Liu, H.; et al. Petrology, mineralogy, and geochemistry of the Ge-rich coal from the Wulantuga Ge ore deposit, Inner Mongolia, China: New data and genetic implications. *Int. J. Coal Geol.* **2012**, *90*, 72–99. [CrossRef]

7. Dai, S.; Jiang, Y.; Ward, C.R.; Gu, L.; Seredin, V.V.; Liu, H.; Zhou, D.; Wang, X.; Sun, Y.; Zou, J.; et al. Mineralogical and geochemical compositions of the coal in the Guanbanwusu Mine, Inner Mongolia, China: further evidence for the existence of an Al (Ga and REE) ore deposit in the Jungar Coalfield. *Int. J. Coal Geol.* **2012**, *98*, 10–40. [CrossRef]

8. Dai, S.; Seredin, V.V.; Ward, C.R.; Jiang, J.; Hower, J.C.; Song, X.; Jiang, Y.; Wang, X.; Gornostaeva, T.; Li, X.; et al. Composition and modes of occurrence of minerals and elements in coal combustion products derived from high-Ge coals. *Int. J. Coal Geol.* **2014**, *121*, 79–97. [CrossRef]

9. Zhou, Y.; Bohor, B.F.; Ren, Y. Trace element geochemistry of altered volcanic ash layers (tonsteins) in Late Permian coal-bearing formations of eastern Yunnan and western Guizhou Provinces, China. *Int. J. Coal Geol.* **2000**, *44*, 305–324. [CrossRef]

10. Dai, S.; Tian, L.; Chou, C.-L.; Zhou, Y.; Zhang, M.; Zhao, L.; Wang, J.; Yang, Z.; Cao, H.; Ren, D. Mineralogical and compositional characteristics of Late Permian coals from an area of high lung cancer rate in Xuan Wei, Yunnan, China: Occurrence and origin of quartz and chamosite. *Int. J. Coal Geol.* **2008**, *76*, 318–327. [CrossRef]

11. Dai, S.; Zhou, Y.; Zhang, M.; Wang, X.; Wang, J.; Song, X.; Jiang, Y.; Luo, Y.; Song, Z.; Yang, Z.; et al. A new type of Nb (Ta)–Zr (Hf)–REE–Ga polymetallic deposit in the late Permian coal-bearing strata, eastern Yunnan, southwestern China: possible economic significance and genetic implications. *Int. J. Coal Geol.* **2010**, *83*, 55–63. [CrossRef]

12. Dai, S.; Li, T.; Seredin, V.V.; Ward, C.R.; Hower, J.C.; Zhou, Y.; Zhang, M.; Song, X.; Song, W.; Zhao, C. Origin of minerals and elements in the Late Permian coals, tonsteins, and host rocks of the Xinde Mine, Xuanwei, eastern Yunnan, China. *Int. J. Coal Geol.* **2014**, *121*, 53–78. [CrossRef]

13. Dai, S.; Zhang, W.; Ward, C.R.; Seredin, V.V.; Hower, J.C.; Li, X.; Song, W.; Wang, X.; Kang, H.; Zheng, L.; et al. Mineralogical and geochemical anomalies of late Permian coals from the Fusui Coalfield, Guangxi Province, southern China: Influences of terrigenous materials and hydrothermal fluids. *Int. J. Coal Geol.* **2013**, *105*, 60–84. [CrossRef]

14. Dai, S.; Zhang, W.; Seredin, V.V.; Ward, C.R.; Hower, J.C.; Song, W.; Wang, X.; Li, X.; Zhao, L.; Kang, H.; et al. Factors controlling geochemical and mineralogical compositions of coals preserved within marine carbonate successions: A case study from the Heshan Coalfield, southern China. *Int. J. Coal Geol.* **2013**, *109*, 77–100. [CrossRef]

15. Dai, S.; Luo, Y.; Seredin, V.V.; Ward, C.R.; Hower, J.C.; Zhao, L.; Liu, S.; Zhao, C.; Tian, H.; Zou, J. Revisiting the late Permian coal from the Huayingshan, Sichuan, southwestern China: Enrichment and occurrence modes of minerals and trace elements. *Int. J. Coal Geol.* **2014**, *122*, 110–128. [CrossRef]

16. Li, B.; Zhuang, X.; Li, J.; Querol, X.; Font, O.; Moreno, N. Geological controls on mineralogy and geochemistry of the Late Permian coals in the Liulong Mine of the Liuzhi Coalfield, Guizhou Province, Southwest China. *Int. J. Coal Geol.* **2016**, *154*, 1–15. [CrossRef]

17. Standardization Administration of China; General Administration of Quality Supervision, Inspection and Quarantine of the China. *Chinese National Standard GB/T 212-2008; Proximate Analysis of Coal*; Standand Press of China: Beijing, China, 2008; pp. 3–5. (In Chinese)

18. Standardization Administration of China; General Administration of Quality Supervision, Inspection and Quarantine of the China. *Chinese National Standard GB/T 214-2007; The Determination Methods of Total Sulfur in Coal*; Standand Press of China: Beijing, China, 2007; pp. 1–5. (In Chinese)

19. Standardization Administration of China; General Administration of Quality Supervision, Inspection and Quarantine of the China. *Chinese National Standard GB/T 215-2003; The Determination Methods of Form Sulfur in Coal*; Standand Press of China: Beijing, China, 2003; pp. 1–5. (In Chinese)

20. International Organization for Standardization. *Methods for the Petrographic Analysis of Bituminous Coal and Anthracite-Part 5: Method of Determining Microscopically the Reflectance of Vitrinite (ISO 7404-5)*; International Organization for Standardization (ISO): Geneva, Switzerland, 2009.

21. Dai, S.; Hower, J.C.; Ward, C.R.; Guo, W.; Song, H.; O'Keefe, J.M.K.; Xie, P.; Hood, M.M.; Yan, X. Elements and phosphorus minerals in the middle Jurassic inertinite-rich coals of the Muli Coalfield on the Tibetan Plateau. *Int. J. Coal Geol.* **2015**, *144*, 23–47. [CrossRef]

22. Standardization Administration of China; General Administration of Quality Supervision, Inspection and Quarantine of the China. *Chinese National Standard GB/T 4633-1997; Determination of Fluorine in Coal*; Standard Press of China: Beijing, China, 1997; pp. 1–5. (In Chinese)

23. ASTM International. *Standard Classification of Coals by Rank*; ASTM D388-12; ASTM International: West Conshohocken, PA, USA, 2012.

24. Standardization Administration of China; General Administration of Quality Supervision, Inspection and Quarantine of the China. *Chinese National Standard GB/T 15224.1-2004; Classification for Quality of Coal-Part 1: Ash*; Standard Press of China: Beijing, China, 2004; pp. 1–2. (In Chinese)

25. Standardization Administration of China; General Administration of Quality Supervision, Inspection and Quarantine of the China. *Chinese National Standard GB/T 15224.2-2004; Classification for Quality of Coal-Part 2: Sulfur Content*; Standard Press of China: Beijing, China, 2004; pp. 1–2. (In Chinese)

26. Dai, S.; Ren, D.; Chou, C.-L.; Finkelman, R.B.; Seredin, V.V.; Zhou, Y. Geochemistry of trace elements in Chinese coals: A review of abundances, genetic types, impacts on human health, and industrial utilization. *Int. J. Coal Geol.* **2012**, *94*, 3–21. [CrossRef]

27. Ketris, M.P.; Yudovich, Y.E. Estimations of Clarkes for Carbonaceous biolithes: World averages for trace element contents in black shales and coals. *Int. J. Coal Geol.* **2009**, *78*, 135–148. [CrossRef]

28. Dai, S.; Seredin, V.V.; Ward, C.R.; Hower, J.C.; Xing, Y.; Zhang, W.; Song, W.; Wang, P. Enrichment of U–Se–Mo–Re–V in coals preserved within marine carbonate successions: Geochemical and mineralogical data from the Late Permian Guiding Coalfield, Guizhou, China. *Miner. Deposita* **2015**, *50*, 159–186. [CrossRef]

29. Dai, S.; Li, D.; Chou, C.-L.; Zhao, L.; Zhang, Y.; Ren, D.; Ma, Y.; Sun, Y. Mineralogy and geochemistry of boehmite-rich coals: new insights from the Haerwusu Surface Mine, Jungar Coalfield, Inner Mongolia, China. *Int. J. Coal Geol.* **2008**, *74*, 185–202. [CrossRef]

30. Dai, S.; Chekryzhov, I.Y.; Seredin, V.V.; Nechaev, V.P.; Graham, I.T.; Hower, J.C.; Ward, C.R.; Ren, D.; Wang, W. Metalliferous coal deposits in East Asia (Primorye of Russia and South China): A review of geodynamic controls and styles of mineralization. *Gondwana Res.* **2016**, *29*, 60–82. [CrossRef]

31. Seredin, V.V.; Dai, S. Coal deposits as potential alternative sources for lanthanides and yttrium. *Int. J. Coal Geol.* **2012**, *94*, 67–93. [CrossRef]

32. Taylor, S.R.; McLennan, S.M. *The Continental Crust: Its Composition and Evolution*; Blackwell Scientific Publications: Palo Alto, CA, USA, 1985; p. 312.

33. Zamanian, H.; Ahmadnejad, F.; Zarasvandi, A. Mineralogical and geochemical investigations of the Mombi bauxite deposit, Zagros Mountains, Iran. *Chem. Erde Geochem.* **2016**, *76*, 13–37. [CrossRef]

34. Fu, X.; Wang, J.; Zeng, Y.; Tan, F.; Feng, X. REE geochemistry of marine oil shale from the Changshe Mountain area, northern Tibet, China. *Int. J. Coal Geol.* **2010**, *81*, 191–199. [CrossRef]

35. Shand, P.; Johannesson, K.H.; Chudaev, O.; Chudaeva, V.; Edmunds, W.M. Rare Earth Element Contents of High pCO_2 Groundwaters of Primorye, Russia: Mineral Stability and Complexation Controls. In *Rare Earth Elements in Groundwater Flow Systems*; Johannesson, K.H., Ed.; Springer: Dordrecht, The Netherlands, 2005; Volume 7, pp. 161–186.

36. Dai, S.; Graham, I.T.; Ward, C.R. A review of anomalous rare earth elements and yttrium in coal. *Int. J. Coal Geol.* **2016**, *159*, 82–95. [CrossRef]

37. Ward, C.R. Minerals in bituminous coals of the Sydney Basin (Australia) and the Illinois Basin (USA). *Int. J. Coal Geol.* **1989**, *13*, 455–479. [CrossRef]

38. Hrinko, V. Technological, chemical, and mineralogical characteristics of bauxites and country rocks near Drienovec. *Miner. Slovaca* **1986**, *18*, 551–555.

39. Spears, D.A. The origin of tonsteins, an overview, and links with seatearths, fireclays and fragmental clay rocks. *Int. J. Coal Geol.* **2012**, *94*, 22–31. [CrossRef]

40. Sahoo, P.K.; Tripathy, S.; Panigrahi, M.K.; Equeenuddin, S.M. Geochemical characterization of coal and waste rocks from a high sulfur bearing coalfield, India: Implication for acid and metal generation. *J. Geochem. Explor.* **2014**, *145*, 135–147. [CrossRef]

41. Finkelman, R.B. Environmental Aspects of Trace Elements in Coal. In *Modes of Occurrence of Environmentally-Sensitive Trace Elements in Coal*; Swaine, D.J., Goodarzi, F., Eds.; Springer: Dordrecht, The Netherlands, 1995; Volume 2, pp. 24–50.

42. Chen, P.; Chai, D. *Sedimentary Geochemistry of Carboniferous Bauxite Deposits in Shanxi Massif*; Shanxi Science and Technology Press: Shanxi, China, 1997; pp. 1–194. (In Chinese)

43. Liu, Y.; Cao, L.; Li, Z.; Wang, H.; Chu, T.; Zhang, J. *Element Geochemistry*; Geological publishing press of Beijing: Beijing, China, 1984; pp. 125–136. (In Chinese)

44. Qian, D.D. *History of China's Deposit Discovery, Guizhou Volume*; Geological Publishing House: Beijing, China, 1996; pp. 177–182. (In Chinese)

45. Wang, D.; Li, P.; Qu, W.; Yin, L.; Zhao, Z.; Lei, Z.; Wen, S. Discovery and preliminary study of the high tungsten and lithium contents in the Dazhuyuan bauxite deposit, Guizhou, China. *Sci. China Earth Sci.* **2013**, *56*, 145–152. [CrossRef]

46. Dai, S.; Ren, D.; Chou, C.-L.; Li, S.; Jiang, Y. Mineralogy and geochemistry of the No. 6 coal (Pennsylvanian) in the Junger coalfield, Ordos basin, China. *Int. J. Coal Geol.* **2006**, *66*, 253–270. [CrossRef]

47. Wilkin, R.T.; Barnes, H.L. Formation processes of framboidal pyrite. *Geochim. Cosmochim. Acta* **1997**, *61*, 323–339. [CrossRef]

48. Dai, S.; Hou, X.; Ren, D.; Tang, Y. Surface analysis of pyrite in the No. 9 coal seam, Wuda Coalfield, Inner Mongolia, China, using high-resolution time-of-flight secondary ion mass-spectrometry. *Int. J. Coal Geol.* **2003**, *55*, 139–150. [CrossRef]

49. Diehl, S.F.; Goldhaber, M.B.; Hatch, J.R. Modes of occurrence of mercury and other trace elements in coals from the warrior field, Black Warrior Basin, Northwestern Alabama. *Int. J. Coal Geol.* **2004**, *59*, 193–208. [CrossRef]

50. Zhang, J.; Ren, D.; Zheng, C.; Zeng, R.; Chou, C.-L.; Liu, J. Trace element abundances in major minerals of Late Permian coals from southwestern Guizhou province, China. *Int. J. Coal Geol.* **2002**, *53*, 55–64. [CrossRef]

51. Dai, S.; Yang, J.; Ward, C.R.; Hower, J.C.; Liu, H.; Garrison, T.M.; French, D.; O'Keefe, J.M.K. Geochemical and mineralogical evidence for a coal-hosted uranium deposit in the Yili Basin, Xinjiang, northwestern China. *Ore Geol. Rev.* **2015**, *70*, 1–30. [CrossRef]

52. Diehl, S.F.; Goldhaber, M.B.; Koenig, A.E.; Lowers, H.A.; Ruppert, L.F. Distribution of arsenic, selenium, and other trace elements in high pyrite Appalachian coals: Evidence for multiple episodes of pyrite formation. *Int. J. Coal Geol.* **2012**, *94*, 238–249. [CrossRef]

53. Dai, S.; Zou, J.; Jiang, Y.; Ward, C.R.; Wang, X.; Li, T.; Xue, W.; Liu, S.; Tian, H.; Sun, X.; et al. Mineralogical and geochemical compositions of the Pennsylvanian coal in the Adaohai Mine, Daqingshan Coalfield, Inner Mongolia, China: Modes of occurrence and origin of diaspore, gorceixite, and ammonian illite. *Int. J. Coal Geol.* **2012**, *94*, 250–270. [CrossRef]

54. Dai, S.; Ren, D.; Li, S.; Chou, C.-L. A discovery of extremely-enriched boehmite from coal in the Junger coalfield, the Northeastern Ordos Basin. *Acta Geol. Sin.* **2006**, *80*, 294–300. (In Chinese)

55. Dai, S.; Yan, X.; Ward, C.R.; Hower, J.C.; Zhao, L.; Wang, X.; Zhao, L.; Ren, D.; Finkelman, R.B. Valuable elements in Chinese coals: A review. *Int. Geol. Rev.* **2016**. [CrossRef]

56. Hower, J.C.; Eble, C.F.; Dai, S.; Belkin, H.E. Distribution of rare earth elements in eastern Kentucky coals: Indicators of multiple modes of enrichment? *Int. J. Coal Geol.* **2016**, *160–161*, 73–81. [CrossRef]

57. Zhao, L.; Dai, S.; Graham, I.; Wang, P. Clay mineralogy of coal-hosted Nb-Zr-REE-Ga mineralized beds from Late Permian strata, eastern Yunnan, SW China: Implications for palaeotemperature and origin of the micro-quartz. *Minerals* **2016**, *6*, 45. [CrossRef]

58. Johnston, M.N.; Hower, J.C.; Dai, S.; Wang, P.; Xie, P.; Liu, J. Petrology and Geochemistry of the Harlan, Kellioka, and Darby Coals from the Louellen 7.5-Minute Quadrangle, Harlan County, Kentucky. *Minerals* **2015**, *5*, 894–918. [CrossRef]

59. Dai, S.; Liu, J.; Ward, C.R.; Hower, J.C.; French, D.; Jia, S.; Hood, M.M.; Garrison, T.M. Mineralogical and geochemical compositions of Late Permian coals and host rocks from the Guxu Coalfield, Sichuan Province, China, with emphasis on enrichment of rare metals. *Int. J. Coal Geol.* **2015**. [CrossRef]

60. Liu, J.; Yang, Z.; Yan, X.; Ji, D.; Yang, Y.; Hu, L. Modes of occurrence of highly-elevated trace elements in superhigh-organic-sulfur coals. *Fuel* **2015**, *156*, 190–197. [CrossRef]

61. Dai, S.; Wang, P.; Ward, C.R.; Tang, Y.; Song, X.; Jiang, J.; Hower, J.C.; Li, T.; Seredin, V.V.; Wagner, N.J.; et al. Elemental and mineralogical anomalies in the coal-hosted Ge ore deposit of Lincang, Yunnan, southwestern China: Key role of N_2-CO_2-mixed hydrothermal solutions. *Int. J. Coal Geol.* **2015**, *152*, 19–46. [CrossRef]

62. Dai, S.; Liu, J.; Ward, C.R.; Hower, J.C.; Xie, P.; Jiang, Y.; Hood, M.M.; O'Keefe, J.M.K.; Song, H. Petrological, geochemical, and mineralogical compositions of the low-Ge coals from the Shengli Coalfield, China: A comparative study with Ge-rich coals and a formation model for coal-hosted Ge ore deposit. *Ore Geol. Rev.* **2015**, *71*, 318–349. [CrossRef]

63. Dai, S.; Li, T.; Jiang, Y.; Ward, C.R.; Hower, J.C.; Sun, J.; Liu, J.; Song, H.; Wei, P.; Li, Q.; et al. Mineralogical and geochemical compositions of the Pennsylvanian coal in the Hailiushu Mine, Daqingshan Coalfield, Inner Mongolia, China: Implications of sediment-source region and acid hydrothermal solutions. *Int. J. Coal Geol.* **2015**, *137*, 92–110. [CrossRef]

64. Eskenazy, G.; Dai, S.; Li, X. Fluorine in Bulgarian coals. *Int. J. Coal Geol.* **2013**, *105*, 16–23.

65. Hower, J.C.; Eble, C.F.; O'Keefe, J.M.K.; Dai, S.; Wang, P.; Xie, P.; Liu, J.; Ward, C.R.; French, D. Petrology, Palynology, and Geochemistry of Gray Hawk Coal (Early Pennsylvanian, Langsettian) in Eastern Kentucky, USA. *Minerals* **2015**, *5*, 592–622. [CrossRef]

66. Dai, S.; Ren, D.; Tang, Y.; Shao, L.; Li, S. Distribution, isotopic variation and origin of sulfur in coals in the Wuda coalfield, Inner Mongolia, China. *Int. J. Coal Geol.* **2002**, *51*, 237–250. [CrossRef]

67. O'Keefe, J.M.K.; Bechtel, A.; Christanis, K.; Dai, S.; DiMichele, W.A.; Eble, C.F.; Esterle, J.S.; Mastalerz, M.; Raymond, A.L.; Valentim, B.V.; et al. On the fundamental difference between coal rank and coal type. *Int. J. Coal Geol.* **2013**, *118*, 58–87. [CrossRef]

68. Goodarzi, F.; Swaine, D.J. *Paleoenvironmental and Environmental Implications of the Boron Content of Coals*; Geological Survey of Canada: Calgary, AB, Canada, 1994; Volume 471, p. 82.

69. Shao, L.; Jones, T.; Gayer, R.; Dai, S.; Li, S.; Jiang, Y.; Zhang, P. Petrology and geochemistry of the high-sulphur coals from the Upper Permian carbonate coal measures in the Heshan Coalfield, southern China. *Int. J. Coal Geol.* **2003**, *55*, 1–26. [CrossRef]

70. Dai, S.; Xie, P.; Jia, S.; Ward, C.R.; Hower, J.C.; Yan, X.; French, D. Enrichment of U-Re-V-Cr-Se and rare earth elements in the Late Permian coals of the Moxinpo Coalfield, Chongqing, China: Genetic implications from geochemical and mineralogical data. *Ore Geol. Rev.* **2016**. [CrossRef]

71. Dai, S.; Ren, D.; Zhou, Y.; Chou, C.-L.; Wang, X.; Zhao, L.; Zhu, X. Mineralogy and geochemistry of a superhigh-organic-sulfur coal, Yanshan Coalfield, Yunnan, China: Evidence for a volcanic ash component and influence by submarine exhalation. *Chem. Geol.* **2008**, *255*, 182–194. [CrossRef]

72. Chou, C.-L. Sulfur in coals: A review of geochemistry and origins. *Int. J. Coal Geol.* **2012**, *100*, 1–13. [CrossRef]

73. Jin, Y.; Fang, R. Early Permian brachiopods from the Kuangshan Formation in Luliang County, Yunnan, with notes on paleogeography of South China during the Liangshan Stage. *Acta Palaeontol. Sin.* **1985**, *24*, 216–228.

74. Zhao, L.; Dai, S.; Graham, I.T.; Li, X.; Liu, H.; Song, X.; Hower, J.C.; Zhou, Y. Cryptic sediment-hosted critical element mineralization from eastern Yunnan Province, southwestern China: Mineralogy, geochemistry, relationship to Emeishan alkaline magmatism and possible origin. *Ore Geol. Rev.* **2016**. [CrossRef]